

# Hydrogen Effects in ECR-Etching of 3C-SiC(100) Mesa Structures

Lars Hiller<sup>1, a</sup>, Thomas Stauden<sup>1, b</sup>, Ricarda M. Kemper<sup>2, c</sup>,  
Jörg K.N. Lindner<sup>2, d</sup>, Donat J. As<sup>2, e</sup> and Jörg Pezoldt<sup>1, f\*</sup>

<sup>1</sup>FG Nanotechnologie, Institut für Mikro- und Nanotechnologien MacroNano<sup>®</sup> and Institut für Mikro- und Nanoelektronik, TU Ilmenau, Postfach 100565, 98684 Ilmenau, Germany

<sup>2</sup>Department Physik, Universität Paderborn, Warburgerstraße 100, 33098 Paderborn, Germany

<sup>a</sup>lars.hiller@tu-ilmenau.de, <sup>b</sup>thomas.stauden@tu-ilmenau.de, <sup>c</sup>rkemper@mail.uni-paderborn.de, <sup>d</sup>lindner@physik.upb.de, <sup>e</sup>d.as@uni-paderborn.de, <sup>f\*</sup>joerg.pezoldt@tu-ilmenau.de

**Keywords:** Plasma etching, electron cyclotron resonance etching, electron beam lithography.

**Abstract.** An anisotropic etching process for mesa structures using fluorinated plasma with hydrogen addition was developed in an electron cyclotron resonance setup. The evolution of the mesa morphology was studied in dependence on the gas composition, the applied bias and the pressure. The achieved side wall slope approached 90° with a negligible trenching. The aspect ratios of the fabricated structure in the developed residue free ECR plasma etching process were between 5 and 20.

## Introduction

3C-SiC grown on Si substrates allows combining the advantages of SiC with the large area abilities of the silicon technology. This makes the fabrication of nanoelectromechanical [1] and nanoelectronic [2] devices feasible. As a special application field 3C-SiC on Si is used as a pseudosubstrate for the growth of other wide band gap materials. The quality of the grown heteroepitaxial layer can be improved if the substrate is patterned with nanostructures [3-5]. This approach was also applied to the growth of 3C-GaN on Si substrates [6].

Generally, to target these application fields, the formation of controlled surface morphologies or lateral structures with dimensions down to sub 100 nm feature sizes is required. Dry etching techniques are the methods of choice to meet the requirements, not only caused by the intrinsic high chemical stability of the SiC, but also driven by the required specific morphology and feature size.

In the past the effect of the temperature, the gas mixture containing reactive gases like SF<sub>6</sub>, NF<sub>3</sub>, CHF<sub>3</sub>, CF<sub>4</sub>, IBr, BCl<sub>3</sub> and Cl<sub>2</sub>, and O<sub>2</sub>, Ar or N<sub>2</sub> additions on the etching rate of SiC have been investigated [7-9]. In these studies hydrogen additions were mainly used to achieve residue free surface morphologies [9]. Most of the studies used inductively coupled plasma (ICP) reactors and were focused on structures with deep trenches for power and MEMS devices. Electron cyclotron resonance (ECR) plasmas were used to fabricate MEMS [11] and NEMS [1].

In this paper, the investigation concentrates on the influence of hydrogen additions to reactive SF<sub>6</sub>/Ar plasmas on the steepness of the side walls of submicrometer 3C-SiC(100) structures. In previous studies the ECR plasma etching was used to achieve free standing III-nitride MEMS-structures [11], NEMS [1] and mesa structures [12] without hydrogen additions. It will be demonstrated that nanosized structures can be fabricated using electron beam lithography and a two layer shadow mask technique in combination with lift-off technique. Compared to the hydrogen free ECR-plasma etching process [12] the steepness of the side wall is improved. Furthermore, the trenching effect near the side walls of the mesa structures is suppressed.

## Experimental

10 μm thick 3C-SiC(100) epitaxial layers grown on 4 inch Si(100) wafers by Novasic<sup>®</sup> were used. After cutting, the samples were cleaned in acetone, isopropanol and DI water using an

ultrasonic excitation. An ALLRESIST<sup>®</sup> PMMA based two resist layer system was used. The different PMMA layers had different thicknesses and sensitivities allowing the creation of a shadow mask with an undercut and edges with low roughness.

The structures were defined with a Raith 150 EBL system at 20 kV acceleration voltage using a 7.5  $\mu\text{m}$  aperture. The layout of the test mask contains an exposure dose variation for areas, lines, dots and different gratings. The exposed samples were developed in AR-600-56 developer for 30 s. After a cleaning step in isopropanol and DI water, the masking material (Ni) was deposited using a LES 250 electron beam evaporation system. The thickness of the deposited materials was 30-70 nm. After lift-off the cleaning with isopropanol and DI water was repeated.

The masked samples were etched in an ECR plasma etching tool. It consists of a turbo molecular pumped box coater type recipient equipped with an 800 W 2.45 GHz downstream ECR plasma source SQ160 from Roth und Rau AG. The mass flow controlled working gases (Ar, O<sub>2</sub>, SF<sub>6</sub>) were fed into the plasma source. The water-cooled 4 inch substrate holder can be charged with DC bias up to -500 V or RF bias by a 13.6 MHz generator up to 100 W. In combination with the large distance of 250 mm between the plasma source and the chuck, these conditions have the potential to vary the etching profile from nearly isotropic profiles as demonstrated in [13] to anisotropic profiles [1, 14]. After loading the samples, the PMMA residues were removed by an oxygen cleaning process at a pressure of  $2.5 \times 10^{-3}$  mbar, an ECR power of 640 W and a DC bias of -100 V. The duration of the removal procedure was 10 min. Subsequently to the cleaning step the etching of the 3C-SiC(100) was carried out. Finally, the nickel mask was removed in HNO<sub>3</sub> at 80°C.

## Results and Discussion

Mesa structures oriented along [100] and [110] directions were fabricated. A typical set of Mesa structures in dependence on the hydrogen addition to the etching gas mixture is shown in Fig. 1 (a, b, c). The morphology of the mesa structure transforms continuously with increasing hydrogen flow. Without hydrogen addition (Fig. 1a) the etch profile consists of an anisotropic part on top of the mesa. With increasing etching depth the side walls develop isotropic like morphology features in form of a slightly elliptic geometry. This effect flattens the steepness of the Mesa sidewalls. At the base of the mesa structure enhanced erosion occurs, evidenced a by clear micro trench development. The increasing cross section and changing sidewall geometry is caused by the tapering effect [15]. Tapering occurs due to side wall reflection of the incident ions. These reflections in turn led to an increased ion density at the bottom near the base of the mesa structure, increasing the physical component of the etching process, causing the formation of micro trenches.

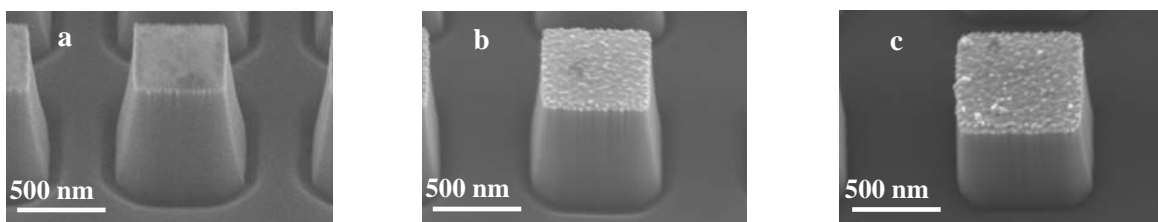


Fig.1 Evolution of the 3C-SiC(100) mesa morphology with Ni mask in dependence on the hydrogen flow in the argon (20 sccm) SF<sub>6</sub> (5 sccm) gas mixture at a pressure of 0.0006 mbar and a bias of -200 V and a platen power of 20 W: (a) 0 sccm H<sub>2</sub>, (b) 2 sccm H<sub>2</sub>, (c) 10 sccm H<sub>2</sub>.

If H<sub>2</sub> is added to the reactive gas mixture the side wall slope increases and the microtrenching reduces continuously. This is demonstrated in Fig 1b and 1c. The increased sidewall slope was independent on the etching time, i.e. no reduction of the sidewall slope and trench formation was observed for higher etching depth. Furthermore, independent on the etching conditions in all cases residue free 3C-SiC(100) surfaces were obtained.

The dependence of the sidewall slope on the H<sub>2</sub> flow in the ECR plasma reactor is given in Fig. 2. As can be seen, H<sub>2</sub> additions to the Ar/SF<sub>6</sub> gas mixture increase the side wall slope of the mesa structures continuously. At H<sub>2</sub> additions above 10 sccm the sidewall slope exceeds the values re-

ported previously [12], where no  $H_2$  was used and the mesa morphology was controlled only by adjusting the plasma pressure and the DC bias (platen power). An increase of the platen power further enhances the side wall steepness (Fig. 2). Beside the side wall slope the  $H_2$  additions affect the etching rate of the 3C-SiC. With increasing  $H_2$  concentration the etching rate decreases, as shown in Fig. 3. A similar effect was observed in case of reactive ion etching, where an etch rate reduction due to  $H_2$  additions was also observed [9]. The trenching and tapering of mesa structures are side effects of the ion bombardment of the silicon carbide mesa sidewall surfaces. Taking into account the etch rate reduction it can be believed that  $H_2$  addition reduces the density of the active fluorine species and charged ions. As a consequence surface charging and the ion reflection probability are reduced. This causes steeper sidewalls at the early stages of the etching process in turn reducing the reflection of the incident ions and therefore the ion density near the bottom of the sidewalls suppressing the trenching. At higher  $H_2$  concentrations the  $H_2$  surface passivation might further reduce the 3C-SiC(100) etch rate.

In Fig. 4 the dependence of the sidewall slope on the plasma pressure is given. The steepness of

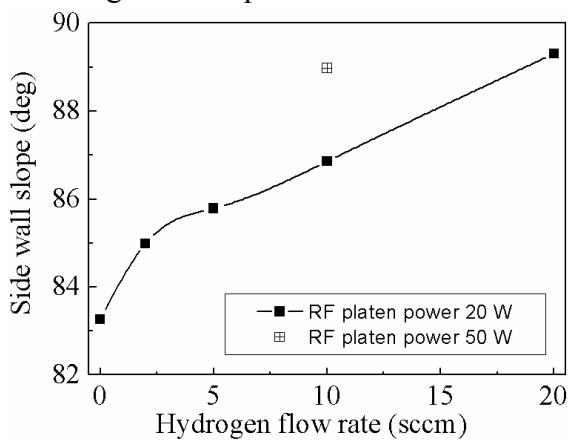


Fig. 2: Side wall slope versus hydrogen addition to the Ar/SF<sub>6</sub> gas mixture (20 sccm Ar, 5 sccm SF<sub>6</sub>, 0.0006 mbar, bias -200 V).

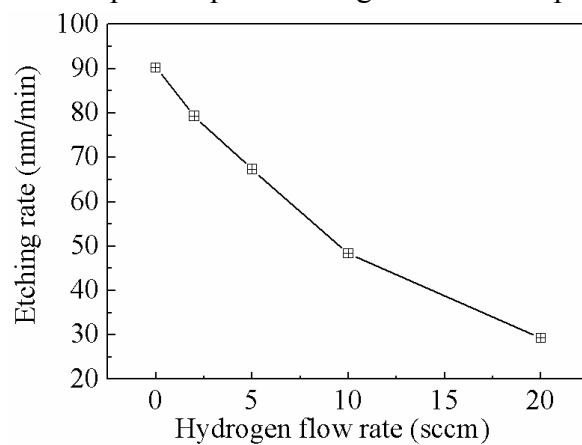


Fig. 3: Etching rate versus hydrogen addition to the Ar/SF<sub>6</sub> gas mixture (20 sccm Ar, 5 sccm SF<sub>6</sub>, 0.0006 mbar, bias -200 V, platen power 20 W).

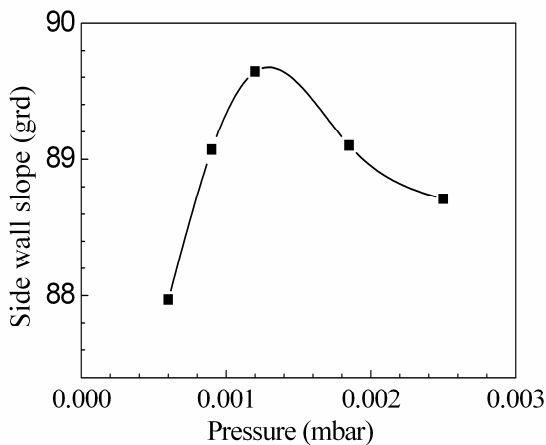


Fig. 4: Side wall slope versus plasma pressure (20 sccm Ar, 5 sccm SF<sub>6</sub>, 10 sccm H<sub>2</sub>, bias -200 V, Platen power 20 W).

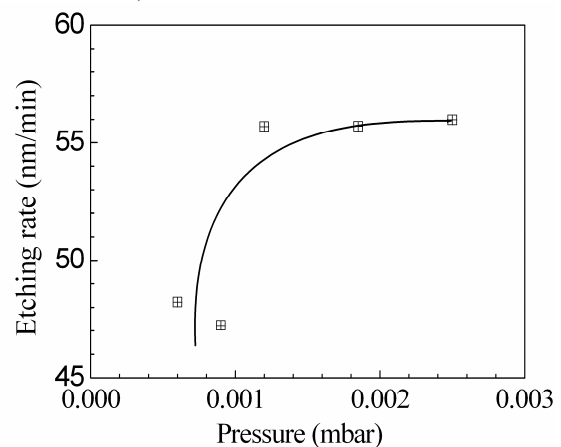


Fig. 5: Etching rate versus plasma pressure (20 sccm Ar, 5 sccm SF<sub>6</sub>, 10 sccm H<sub>2</sub>, bias -200 V, Platen power 20 W).

the side wall slope displays a maximum between 0.001 and 0.002 mbar. The obtained values are close to vertical sidewalls with a deviation from the surface normal less than 1°. Increased overall pressure allows increasing the etching rate (Fig. 5). In this pressure range with the highest side wall slope the etching rate saturates. The highest sidewall steepness corresponds to the maximum etch rate in the pressure dependence of approximately 55 nm/min. Therewith, hydrogen addition in

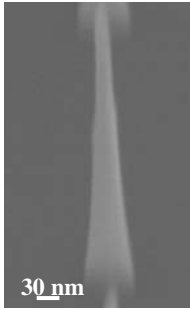


Fig. 6:  
Fabricated  
nanostructure

combination with pressure variation give the ability to optimize the mesa morphology and etching rate of 3C-SiC(100) in fluorinated ECR-plasmas.

Furthermore, the carried out investigations revealed that the side wall roughness is mainly determined by the mask erosions and the evolution of the grain size during the etching process of the used masking material. As a consequence metals forming sub nanometer grains and keeping them during etching have to be used if smooth steep side walls are required. Under our experimental conditions nickel fulfills the requirements. The developed processes allowed the fabrication of sub 100 nm structures with aspect ration up to 20. A columnar structure with top diameter of 20 nm and a height of 400 nm is shown in Fig. 6.

### Summary

Hydrogen additions and pressure variations allow the improvement of the mesa structure sidewall morphology and the optimization of the 3C-SiC(100) etch rate. It is demonstrated that adjusting these two parameters nearly vertical side walls can be achieved.

### References

- [1] M. Hofer, Th. Stauden, I.W. Rangelow, J. Pezoldt, Mater. Sci. Forum 645-648 (2010) 841-844.
- [2] Y. Ikoma, T. Tada, K. Uchiyama, F. Watanabe, T. Motooka, Solid State Phenomena 78-79 (2001) 157-164.
- [3] M.E. Okhuysen, M.S. Mazzola, Y.-H. Lo, Mater. Sci. Forum, 338-342 (2000) 305-308.
- [4] Y. Fu, F. Yun, Y.T. Moon, J.Q. Xie, Ü. Özgür, S. Dogan, H. Morkoc, C.K. Inoki, T.S. Kuan, I. Zhou, D.J. Smith, Appl. Phys. Lett. 86 (2005) 043108/1-043108/3.
- [5] D. Zubia, S.H. Zaidi, S.R.J. Brueck, S.D. Hersee, Appl. Phys. Lett. 76 (2000) 858-860.
- [6] R.M. Kemper, L. Hiller, T. Stauden, J. Pezoldt, K. Duschik, T. Niendorf, H.J. Maier, D. Meertens, K. Tillmann, D.J. As, J.K.N. Lindner, J. Cryst. Growth 378 (2013) 291-294.
- [7] G. McDaniel, J.W. Lee, E.S. Lambers, S.J. Pearton, P.H. Holloway, F. Ren, J.M. Grow, M. Bhaskaran, R.G. Wilson, J. Vac. Sci. Technol. A 15 (1997) 885-889.
- [8] J.J. Wang, E.S. Lambers, S.J. Pearton, M. Ostling, C.-M. Zetterling, J.M. Grow, F. Ren, R.J. Shul: Solid-State Electronics, 42 (1998) 2283-2288.
- [9] P. Yih, A.J. Steckl, J. Electrochem. Soc. 140 (1993) 1813-1824.
- [10] Th. Stauden, F. Niebelschütz, K. Tonisch, V. Cimalla, G. Ecke, Ch. Haupt, J. Pezoldt, Mater. Sci. Forum, 600-603 (2009) 651-654.
- [11] Ch. Förster, V. Cimalla, M. Stubenrauch, C. Rockstuhl, K. Brueckner, M. Hein, J. Pezoldt, O. Ambacher, Mater. Sci. Forum 527-529 (2006) 1111-1114.
- [12] L. Hiller, Th. Stauden, R.M. Kemper, J.K.N. Lindner, D.J. As, J. Pezoldt, Mater. Sci. Forum 717-720 (2012) 901-904.
- [13] F. Niebelschütz, Th. Stauden, K. Tonisch, J. Pezoldt, Mater. Sci. Forum 645-648 (2010) 849-852.
- [14] Ch. Förster, V. Cimalla, R. Kosiba, G. Ecke, P. Weih, O. Ambacher, J. Pezoldt, Mater. Sci. Forum 457-460 (2004) 821-824.
- [15] H. Dimigen, H. Lühje, Philips Techn. Rev. 35 (1975) 199-208.